matrix as

$$\mathbf{M}(y)=\mathbf{M}_a+y\mathbf{M}_b, \quad (A.17)$$

where $\mathbf{M}_a$ arises from the A-B interactions, $y\mathbf{M}_b$ from the B-B interactions ($\mathbf{M}_a$ and $\mathbf{M}_b$ are independent of y). The eigenvalue equation, in vector notation, is

$$\mathbf{M}(y)\mathbf{U}(y)=m(y)\mathbf{U}(y).$$

Clearly

$$m(y)=(\mathbf{U}(y),\mathbf{M}\mathbf{U}(y))/(\mathbf{U}(y),\mathbf{U}(y)).$$

Letting prime indicate differentiation with respect to y, we have

$$m'(y)=(\mathbf{U}(y),\mathbf{M}_b\mathbf{U}(y))/(\mathbf{U}(y),\mathbf{U}(y)). \quad (A.18)$$

But Eq. (7) shows that the B-B interaction is negative semidefinite; since the right-hand side of (A.18) represents the B-B interaction energy for some set of deviations, it follows that

$$\frac{\partial}{\partial y}m_\nu(\mathbf{k})\leqslant 0, \quad \text{all } \nu, \mathbf{k}. \quad (A.19)$$

PHYSICAL REVIEW VOLUME 119, NUMBER 5 SEPTEMBER 1, 1960

Magnetic Properties of Mn_3O_4 and the Canted Spin Problem*

KIRBY DWIGHT AND NORMAN MENYUK
Lincoln Laboratory, Massachusetts Institute of Technology, Lexington, Massachusetts

(Received April 11, 1960)

The magnetic properties of single crystals of hausmannite (Mn_3O_4) have been investigated between 4.2°K and the ferrimagnetic Curie point at 41.9°K. The c axis was found to be the hard direction of magnetization and the c plane was found to possess considerable anisotropy, with respective anisotropy fields of about 10^5 oe and 10^4 oe. These anisotropy energies decreased slowly with increasing temperature, whereas the coercive force at 15°K was about an order of magnitude less than at 4.2°K. The spontaneous magnetization is 1.85 μ_B/molecule, which agrees with previous polycrystalline values when the observed anisotropies are taken into account. However, several of the observed properties of hausmannite disagree, some quantitatively and others qualitatively, with calculations based on the Yafet-Kittel theory. It is concluded that the concept of canted spins is essentially correct, but that the specific Yafet-Kittel model involves oversimplifications which limit its applicability.

I. INTRODUCTION

CONSIDERABLY more information can be obtained from studies of the magnetic properties of single crystals than from those made with polycrystalline samples. The magnetic anisotropy, which is a sensitive indicator of magnetic symmetry and of changes in that symmetry, can be determined in detail only by measurements on single crystals. Furthermore, an accurate determination of the magnetization of a single crystal can be made independently of the crystalline anisotropy by applying the external field along an easy direction. In polycrystalline samples, however, anisotropy has the effect of reducing the apparent magnetic moment. This effect can be important for materials with large anistropy.

We have investigated the magnetic properties of single-crystal samples of hausmannite (Mn_3O_4),[1] which is known to become ferrimagnetic at about 42°K.[2] Our measurements show that the c axis is a hard magnetization direction and that the c plane also possesses considerable anisotropy, the respective anisotropy fields being approximately 10^5 oe and 10^4 oe. The temperature variations of both these anisotropy energies are small. On the other hand, the coercive force at about 15°K is an order of magnitude less than the 2650 oe observed at 4.2°K. We find the spontaneous magnetization to be 1.85 μ_B/molecule, which is greater than the values 1.4 μ_B/molecule[3] and 1.56 μ_B/molecule[4] previously measured for polycrystalline samples. Both of the latter values are low because of the anisotropy effect, and can be brought into good agreement with our present value by a correction calculated from our anisotropy data. However, our present value is also less than the 3.0 μ_B/molecule predicted by the Néel model of ferrimagnetism.

Many other materials with spinel structure exhibit smaller spontaneous magnetizations than predicted.[5] The Yafet-Kittel theory[6] of spin angles was introduced to account for such reduced moments. Although hausmannite has a cubic spinel structure above 1170°C,

* The work reported in this paper was performed by Lincoln Laboratory, a center for research operated by Massachusetts Institute of Technology with the joint support of the U. S. Army, Navy, and Air Force.

[1] Obtained through the courtesy of the New York Museum of Natural History.

[2] A. S. Borovik-Romanov and M. P. Orlova, J. Exptl. Theoret. Phys. (U.S.S.R.) **32**, 1255 (1957) [translation: Soviet Phys.—JETP **5**, 1023 (1957)].

[3] D. G. Wickham and W. J. Croft, J. Phys. Chem. Solids **7**, 351 (1958).

[4] I. S. Jacobs, J. Appl. Phys. **30**, 301S (1959).

[5] E. W. Gorter, Philips Research Repts. **9**, 295, 321, 403 (1954).

[6] Y. Yafet and C. Kittel, Phys. Rev. **87**, 290 (1952).

it becomes tetragonally distorted[7] at lower temperatures, as was explained by Goodenough and Loeb.[8] This distortion must affect the magnetic properties in some manner, but does not detract from the applicability of the Yafet-Kittel model. To the contrary, Kaplan has recently shown[9] that their configuration can only be stable in a distorted spinel.

When our numerical values for the spontaneous magnetization, anisotropy, and ferrimagnetic Curie temperature are substituted into expressions derived straightforwardly from the Yafet-Kittel model, a distinct discrepancy appears. This discrepancy was also implicit in the work of Jacobs[10] on polycrystalline Mn_3O_4, but was overshadowed by his high-field evidence for canted spins and by Kasper's[11] success in fitting neutron-diffraction data with a modified ordering of Yafet-Kittel angles. However, neither the temperature variation of the coercive force nor the peculiar remagnetization effects described in this paper can be explained within the framework of the Yafet-Kittel model. Moreover, this model cannot even account for the orthorhombic doubling of the unit cell observed by Kasper,[11] since the doubled configuration is just one element in a degenerate set of ground states. These facts add greatly to the significance of the discrepancy mentioned above.

There is considerable experimental evidence showing that the concept of canted spins is essentially correct in a number of different materials.[10–13] Nevertheless, some confusion concerning the details of the Yafet-Kittel theory still remains. In particular, Prince[13] found affirmative evidence for ordered angles in copper chromite, whereas Pickart and Nathans[14,15] found no such evidence in the nickel-iron chromite and manganese-iron chromite systems. Furthermore, as noted above, neither our findings nor Kasper's doubling of the unit cell[11] can be explained by the Yafet-Kittel theory, although hausmannite does possess canted spins.[10,11] These experimental discrepancies are attributable to the sublattice restrictions of the specific Yafet-Kittel model, which limit its applicability.

II. SAMPLE CONSIDERATIONS: ANALYSIS BY CURIE POINT COMPARISON

Single crystals of hausmannite occur in nature as small pyramids growing out of certain rocks.[16] They are quite rare, and can be found only in a few scattered localities, such as at Ohrenstock near Ilmenau, Thuringia, in Germany. Two hausmannite pyramids[1] from this deposit were examined by x rays, which showed them to be good, untwinned single crystals. Both pyramids were oriented by their x-ray Laue patterns[17] and were sliced, one of them parallel to the bc tetragonal (100) plane, the other parallel to the (001) plane.[18] The relative orientations of these two planes are shown in Fig. 1. Our samples consisted of small disks (approximately 0.100 inch in diameter and 0.020 inch thick) cut from the oriented slices by a Raytheon ultrasonic machine tool.

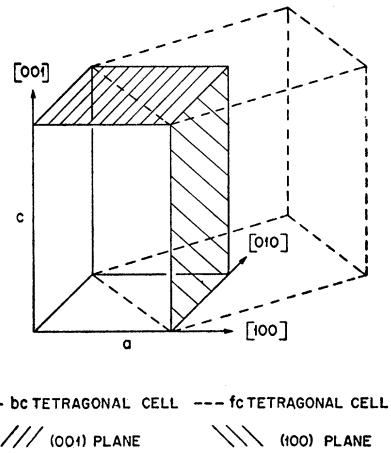

Fig. 1. The relationship between the bc tetragonal unit cell and the fc tetragonal cell (tetragonally distorted fcc cell). The lattice parameters for hausmannite are: $a=5.75$ A and $c/a=1.638$. The sample orientations are indicated by the shaded planes.

The question of chemical composition is particularly important, since both our samples could not be obtained from the same crystal. A complete chemical analysis was impossible for want of material, and for the same reason the sensitivity of an ammonium thiocyanate color test for iron[19] failed at 0.1%. The iron content of our crystals was definitely below this value.

Dana[16] lists two analyses for different hausmannite crystals from Ilmenau, Thuringia. One of these crystals was very pure Mn_3O_4, with only 0.3% impurities (Ba and Si). The other contained 6.9 wt % Zn as the major impurity, with about 0.2% Fe, 0.1% Ca, 0.2% Si, and 0.3% K and Na combined. The absence of iron in our samples indicates that their analysis would probably be of the first type, i.e., pure Mn_3O_4. Furthermore, the presence of Zn as the only major impurity in crystals from Ilmenau implies that our samples' purity could be established through magnetic analysis, since the presence of zinc on spinel A-sites has a marked effect upon the Curie temperature.

[7] F. C. Romeijn, Philips Research Repts. **8**, 304 (1953).
[8] J. B. Goodenough and A. L. Loeb, Phys. Rev. **98**, 391 (1955).
[9] T. A. Kaplan, Phys. Rev. **116**, 888 (1959).
[10] I. S. Jacobs, J. Phys. Chem. Solids **11**, 1 (1959).
[11] J. S. Kasper, Bull. Am. Phys. Soc. **4**, 178 (1959).
[12] P. L. Edwards, Phys. Rev. **116**, 287 (1959).
[13] E. Prince, Acta Cryst. **10**, 554 (1957).
[14] S. J. Pickart and R. Nathans, Phys. Rev. **116**, 317 (1959).
[15] S. J. Pickart and R. Nathans, Bull. Am. Phys. Soc. **3**, 231 (1958).
[16] C. Palache, H. Berman, and C. Frondel, *Dana's System of Mineralogy* (John Wiley & Sons, Inc., New York, 1944), 7th ed., Vol. 1, pp. 712–715.
[17] We are indebted to J. W. Sanchez of Lincoln Laboratory for the x-ray orientation of the crystals.
[18] Throughout this paper we shall refer all directions and planes to the crystallographic bc tetragonal unit cell rather than to the fc cell, unless otherwise stated. Figure 1 shows the relationship between these two descriptions. In particular, the bc tetragonal (100) is identical with the fc tetragonal or cubic (110).
[19] Made by E. R. Whipple.

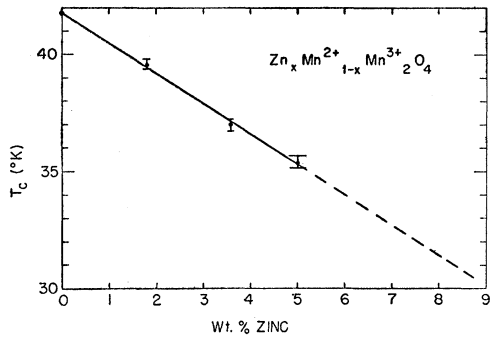

FIG. 2. The dependence of the Curie temperature upon zinc concentration in $Zn_xMn_{1-x}{}^{2+}Mn_2{}^{3+}O_4$. Weight percent $\cong 28.4\,x$.

The ferrimagnetic Curie points of our samples were determined from graphs of magnetization versus temperature plotted automatically by a vibrating-coil magnetometer,[20] using an experimental arrangement similar to that described elsewhere.[21] The external fields applied to the samples were kept small in order to minimize error due to short range order. The temperature signal was obtained from a calibrated Leeds and Northrup platinum resistance thermometer in good thermal contact with the sample, as shown by the lack of appreciable hysteresis between warming and cooling curves. Similar determinations were carried out for polycrystalline samples[22] of pure Mn_3O_4 and of Mn_3O_4 with 1.8±0.1, 3.6±0.1, and 5.0±0.2 wt % zinc additions, with the results shown in Fig. 2.

We found the ferrimagnetic Curie temperature of pure Mn_3O_4 to be 41.8±0.1°K, in good agreement with the value of 42.5°K obtained by Borovik-Romanov.[2] The (001) sample became ferrimagnetic at 41.95±0.1°K, and the (100) sample at 41.2±0.1°K. In comparison with these values, the samples with 1.8±0.1, 3.6±0.1, and 5.0±0.2 wt % Zn addition had Curie points of 39.6±0.2°K, 37.0±0.2°K, and 35.4±0.4°K, respectively. Thus our (001) and (100) samples appear to contain less than 0.1% and 0.5% Zn, respectively.

A third single-crystal hausmannite pyramid[23] from Ilmenau, Thuringia, was examined by x-ray fluorescence by E. P. Warekois, who found zinc to be the major impurity, with other elements also present in smaller quantities. Furthermore, its ferrimagnetic Curie temperature was found to be about 31.8±0.2°K, which indicates about 7.7 wt % zinc. This example of the second type of chemical composition of Ilmenau crystals described in Dana[16] substantiates the dichotomy reported there. Having inferred that hausmannite crystals from Ilmenau are of two distinct types with zinc as the major impurity, we conclude that the type-one analysis does indeed represent a good approximation to the composition of our samples, i.e., that they do consist of reasonably pure Mn_3O_4.

[20] K. Dwight, N. Menyuk, and D. O. Smith, J. Appl. Phys. **29**, 491 (1958).
[21] N. Menyuk and K. Dwight, Phys. Rev. **112**, 397 (1958).
[22] Prepared by D. G. Wickham of Lincoln Laboratory.
[23] Obtained through the courtesy of the Peabody Museum of Harvard University.

III. EXPERIMENTAL RESULTS AT 4.2°K

A. Anisotropy in the (100) Plane

Investigation of the (100) sample in an external field of 11 000 oe at 4.2°K showed that hausmannite is a magnetically hard material. The maximum available field was able to fully magnetize the sample in one direction only, and only a tenth as much magnetization could be obtained at right angles to this direction. An x-ray determination of these two orientations[17] established the [001] (tetragonal c axis) to be the hard direction of magnetization.

To measure the anisotropy, a large external field was initially applied along the easy [010] direction and the spontaneous magnetization M_s was determined. The single-domain sample was then rotated, and the apparent magnetizations M were measured with a known field applied along several other directions. Since the rotational model is valid under these conditions, the apparent moment is given by:

$$M/M_s=\cos(\vartheta_c-\varphi_c), \tag{1}$$

where the magnetization and the applied field make angles of ϑ_c and φ_c, respectively, with the c axis. φ_c is known, and so ϑ_c can be calculated from the measured values of M/M_s.

Since hausmannite possesses twofold magnetic symmetry in the (100) plane, its anisotropy energy can be expressed in the uniaxial form and

$$E_c=E_{Kc}+E_H=K_c\sin^2\vartheta_c-HM_s\cos(\vartheta_c-\varphi_c). \tag{2}$$

Equilibrium in an external field then requires that

$$0=\partial E_c/\partial\vartheta_c=K_c\sin 2\vartheta_c-HM_s\sin(\varphi_c-\vartheta_c). \tag{3}$$

Substitution of our experimental data into Eq. (3) gives values of K_c/M_s between -3×10^4 oe and $-\infty$, with a most probable value of -5×10^4 oe. The range is asymmetrical because of the functional forms of Eqs. (1) and (3). It arises from extreme variations of the order of ±0.03 in our values for M/M_s, and reflects our inability to move the magnetization more than a few degrees away from its easy direction. Using the magnetization value given below (see IIID), it follows that $K_c\approx-10^7$ ergs/cc.

B. Anisotropy in the (001) Plane

Relatively small external fields were able to saturate the (001) sample in two orientations 90° apart. X-ray examination[17] showed these directions of easy magnetization to be the bc tetragonal [100] and [010] axes. However, when the sample is first saturated along one of these directions, fields greater than 4000 oe

are required to remagnetize it along the other direction. Furthermore, the realignment of magnetization is a slow process requiring over an hour at 4500 oe, and several minutes in fields of 10 000 oe. This and other peculiarities in the dynamic behavior of hausmannite will be the subject of a later investigation.

Although all directions in the (001) plane are relatively "easy" compared to the c axis, we found considerable anisotropy to be present within this plane. Its magnitude was calculated from measured ratios of apparent to saturation magnetizations for different sample orientations in various external fields. The sample was cooled through its ferrimagnetic Curie point with a field of 10 000 oe applied along an easy direction, and was never rotated more than 35° away from this direction. These precautions make it reasonable to apply the rotational model to our findings.

Kasper's neutron diffraction study[11] demonstrated hausmannite to possess orthorhombic magnetic symmetry in which the bc tetragonal unit cell is doubled along a [100] direction. If energy can be gained by this doubling, then the 90° remagnetization process described above can be interpreted as a rearrangement of the magnetic symmetry against some energy barrier. Our experimental precautions were such as to preserve a fixed magnetic arrangement, and hence a uniaxial type of anisotropy is to be expected. Equations (1)–(3) should therefore apply, with ϑ_c and φ_c replaced by the angles ϑ_a and φ_a which now are referred to the easy direction in the (001) plane.

According to this model, our small-angle data leads to the value of 5950±350 oe for K_a/M_s. However, additional data was obtained by reducing the external field to zero, rotating the sample 90°, and then gradually increasing the field. The magnetic arrangement should remain unchanged until a "coercive force" is reached, and the uniaxial model should apply up to that point. The above value of K_a/M_s disagrees with this data.

In order to fit both the small-angle and 90° data, it is necessary to include the second-order anisotropy term, i.e.,

$$E_{Ka}=K_a \sin^2\vartheta_a+K_a' \sin^4\vartheta_a. \quad (4)$$

The small-angle data then combines K_a and K_a', so that

$$G/M_s\equiv K_a/M_s+2(K_a'/M_s)\sin^2\vartheta_a = H[\sin(\varphi_a-\vartheta_a)]/\sin 2\vartheta_a. \quad (5)$$

For $\varphi_a=25°$ and $H=5500$ oe, this yields

$$G/M_s=K_a/M_s+(0.0332\mp 0.0028)K'_a/M_s = (5950\pm 350) \text{ oe},$$

where the uncertainties arise from a probable error in M/M_s of 0.15%. Consequently the 90° data leads to estimated values of $K_a/M_s=4800\pm 300$ oe and $K_a'/M_s=34\,000\mp 10\,000$ oe, so that multiplication by our value of M_s (see IIID) yields $K_a=(1.06\pm 0.07)\times 10^6$ ergs/cc and $K_a'=(7.5\mp 2)\times 10^6$ ergs/cc. Theoretical curves based on these values are compared with typical data in Fig. 3, which shows the agreement to be good. Alternatively, if fourfold anisotropy symmetry is assumed and its magnitude is determined from the small-angle data, then the theoretical curve does not agree with the 90° data, as indicated by the dashed line in Fig. 3. In particular, the magnetization could readjust by rotation at fields considerably smaller than the observed "coercive force." Thus our data shows the anisotropy symmetry to be uniaxial in the (001) plane, reinforcing Kasper's observation of orthorhombic doubling.[11]

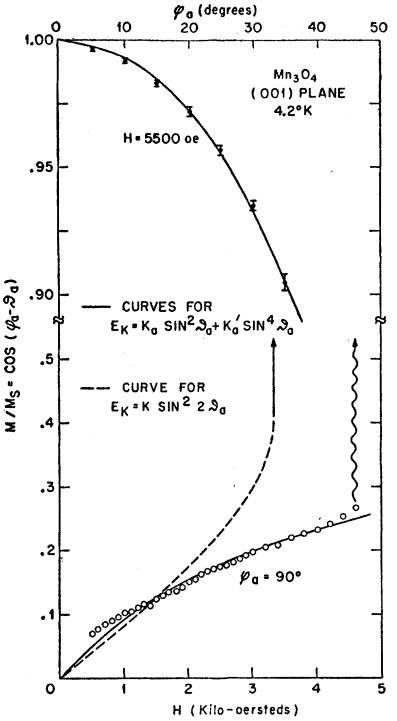

Fig. 3. Experimental values for M/M_s measured at 4.2°K in the (001) plane at various angles from the magnetically easy [100] direction. The solid curves show that the data can be closely fitted by the uniaxial anisotropy given in Eq. (4). The curve shows that the 90° data cannot be reconciled to a fourfold anisotropy fitted to the small-angle data.

C. Coercive Force

It was impossible to obtain good quasi-static $B-H$ loops because of the dynamic behavior described above. Figure 4 shows data typical of both samples. Because of the peculiar dynamics, this data shows that the coercive force for magnetization reversal is probably less than 2800 oe. By waiting for longer times at fields between 2000 and 2800 oe and extrapolating the time dependence, we found that the magnetization could eventually (after about three hours) be reduced to zero by a field of 2650 oe, which we will call the 180° coercive force. The apparent coercivity of 16 000 oe obtained by Jacobs[4,10] with pulsed-field techniques probably resulted

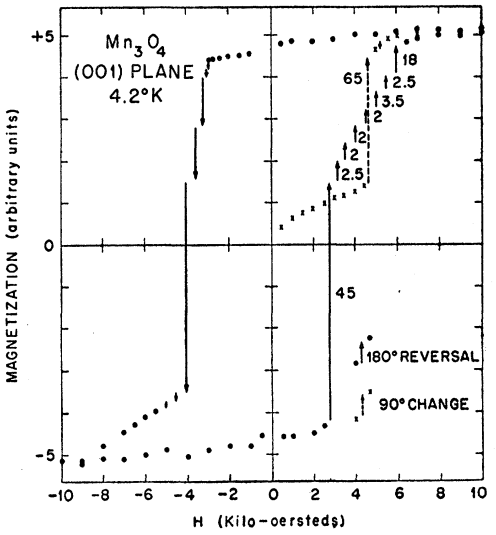

FIG. 4. Dependence of the magnetization upon fields applied along an easy direction at 4.2°K. Data for a 180° field reversal is shown by solid points and solid arrows. Data for a 90° remagnetization is indicated by crosses and dashed arrows. The numbers beside the arrows show the length of time, in minutes, required for the magnetization to change by the indicated amount.

from the dynamic behavior, even larger fields being required for reversal by rotation according to the anisotropy energies given in IIIB.

The 90° data is included in Fig. 4. Once the (001) sample is magnetized along one easy direction, a field of about 4600 oe is required to remagnetize it (after an hour and a half) along the other. The magnetic symmetry of hausmannite has been shown to be orthorhombic with uniaxial anisotropy in the (001) plane. Hence 4600 oe represents the "coercive force" required to overcome the energy barrier between the two equally possible magnetic arrangements at 4.2°K.

D. Spontaneous Magnetization

A field of 10 000 oe was used to compare the magnetic moments of the two hausmannite samples with that of a polycrystalline nickel standard. These measurements yielded $1.87\pm0.02\ \mu_B$/molecule for both samples, based on a saturation moment for nickel of 0.604 μ_B/molecule which was adjusted for the extrapolation from 10 000 oe to an infinite field. The magnetization was then calculated to be 221 cgs/cc by using the theoretical density of 4.84 g/cc. Although this magnetization value was obtained at 10 000 oe, Fig. 4 shows it to be a good approximation to the spontaneous magnetization.

Previous determinations were made with polycrystalline samples, which consist of randomly oriented crystallites. If we neglect the anisotropy within the easy plane, then the angle between the magnetic moment of a crystallite and an applied field will be $(\vartheta_c-\varphi_c)$ as defined in IIIA. The equilibrium condition relating ϑ_c to φ_c is given by Eq. (3), and the magnitude of any individual moment will be $M_s+\chi_m H\cos(\vartheta_c-\varphi_c)$, where χ_m is the molecular susceptibility. The apparent moment is the average component of the individual moments along the applied field, and can be expressed as

$$M=\int_0^{\pi/2}[M_s+\chi_m H\cos(\vartheta_c-\varphi_c)]\times\cos(\vartheta_c-\varphi_c)\sin\varphi_c d\varphi_c. \quad (6)$$

Jacobs polycrystalline data[4,10] shows apparent magnetic moments of 1.70 μ_B and 1.99 μ_B at 45 000 oe and 135 000 oe, respectively. Numerical integration of Eq. (6) gives $M=0.900M_s+37\,000\chi_m$ at the former field, and $M=0.973M_s+128\,000\chi_m$ at the latter. Substitution of the experimental values then yields $\chi_m=1.72\times10^{-6}\ \mu_B$/oe and $M_s=1.82\ \mu_B$. The susceptibility term would reduce our value to $1.85\pm0.02\ \mu_B$, so that good agreement is obtained by using our most probable value for K_c.

A similar correction raises our original polycrystalline determination[3] of 1.4 μ_B/molecule at 10 000 oe to 1.86 μ_B. In this calculation, the anisotropy within the "easy" plane and an approximation to the coercivity effects had to be included because of the smaller applied field.

IV. VARIATIONS WITH TEMPERATURE

The dependence of magnetization upon temperature is illustrated in Fig. 5. The indicated Curie point was obtained from low-field data.

Although our present data on the temperature variation of the coercive force is insufficient to define a functional relationship, it clearly demonstrates a decrease from 2650 oe at 4.2°K to 300 oe by about 15°K. This order-of-magnitude change is in qualitative

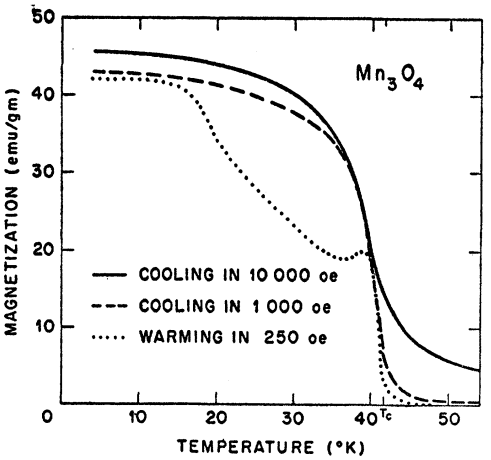

FIG. 5. Dependence of the magnetization upon temperature for various fields applied along the easy direction. The dotted curve falls away from the others at about 16°K because 250 oe was less than the demagnetizing field of our sample. However, the pronounced hump just below the Curie point is anomalous.

agreement with Jacobs' findings,[4,10] from which he infers a similar rapid decrease in the anisotropy energy. Such an inference is normally reasonable, but proves to be erroneous in the case of hausmannite.

The small-angle technique was used to evaluate G in Eq. (5) at several evaluated temperatures, with the results shown in Fig. 6. Classical theory[24] was used to calculate the temperature variations of the uniaxial anisotropies K_a and K_a' separately. These variations were then combined to give the solid curve in Fig. 6 which indicates qualitative agreement with our data. It is significant that the anisotropy remains essentially constant over the temperature range 4.2°K–20°K, whereas the coercive force decreases by over an order of magnitude.

Similar attempts were made to determine K_c at 30°K and 38°K. As discussed earlier in connection with the 4.2°K measurement, accurate values for K_c could not be obtained because the available fields were much smaller than the anisotropy field. Within the uncertainty of our results, there was no indication of a marked decrease in K_c/M_s with increasing temperature. The presumption is that the temperature dependence of the anisotropy energy in the (100) plane is qualitatively similar to that found in the (001) plane.

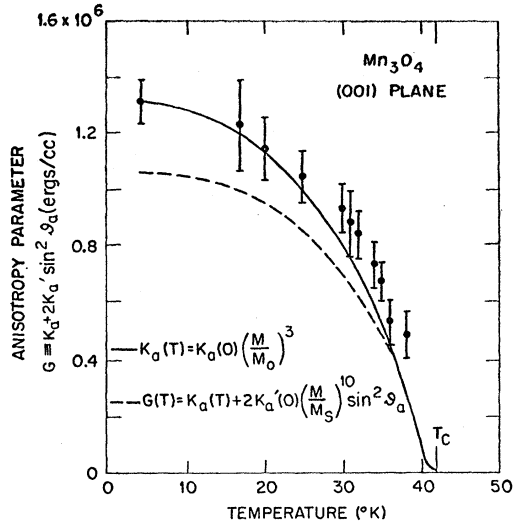

FIG. 6. Dependence of the anisotropy energy upon temperature. The anisotropy parameter G of Eq. (5) was measured by the small-angle technique, with $\varphi_a=25°$ and $H=5000$ oe. The temperature variation of K_a and K_a' were calculated from classical theory. The dashed curve shows the results for the K_a component, and the solid curve gives the total variation for G.

V. DISCUSSION

An adequate theoretical explanation for the behavior of hausmannite must lead to an understanding of many unusual magnetic properties, e.g.: The low value of saturation mangetization, the high-field susceptibility,[4,10] the strong temperature dependence of the coercive force relative to that of the magnetic anisotropy, the orthorhombic doubling of the tetragonal unit cell,[11] and the peculiar dynamic behavior. It must also be consistent with the ferrimagnetic and asymptotic[2,25] Curie points. The first two features suggest an explanation in terms of Yafet-Kittel angles.[10] However, it will be shown that a molecular field calculation based on the Yafet-Kittel theory indicates inconsistency between the saturation moment and the Curie points. The analysis given here is patterned closely after that made by Lotgering,[26] and his notation is adopted throughout this discussion.

In the molecular field calculation of Yafet and Kittel,[6] the minimum energy can be obtained with several distinct spin configurations. Because of this degeneracy, the six spinel sublattices can be reduced to four magnetic subsystems. These correspond to two possible moments, $\mathbf{a}_1$ and $\mathbf{a}_2$, for the A-sites and two possible moments, $\mathbf{b}_1$ and $\mathbf{b}_2$, for pairs of B-sites. Within the framework of triangular spin arrangements, this reduction to four magnetic subsystems remains valid even after tetragonal distortion and orthorhombic doubling of the bc tetragonal unit cell, as shown in Appendix I. Consequently, the Lotgering analysis[26] can be applied to hausmannite. Appendix I shows that the molecular fields, as given by Eq. (A-1), can be rewritten for the four magnetic subsystems in terms of a modified Lotgering notation. Then the molecular fields acting on the A_i and B_i systems become[26]

$$\begin{aligned}\mathbf{h}_{Ai}&=-n[-\alpha\mathbf{a}_i+\alpha\mathbf{A}+\mathbf{B}],\\ \mathbf{h}_{Bi}&=-n[-\tfrac{1}{2}\beta'\mathbf{b}_i+\mathbf{A}+\beta\mathbf{B}],\end{aligned}\tag{7}$$

where $\mathbf{A}$ and $\mathbf{B}$ are the resultant moments of the two A and two B subsystems, respectively, and the interaction strengths are as defined in Appendix I. The exchange energy is then

$$\begin{aligned}E_{\rm ex}&=-\tfrac{1}{2}[\mathbf{a}_1\cdot\mathbf{h}_{A1}+\mathbf{a}_2\cdot\mathbf{h}_{A2}+\mathbf{b}_1\cdot\mathbf{h}_{B1}+\mathbf{b}_2\cdot\mathbf{h}_{B2}],\\ &=n[\alpha\mathbf{a}^2-\tfrac{1}{2}\beta'\mathbf{b}^2+2\mathbf{a}\cdot\mathbf{B}+\tfrac{1}{2}\beta\mathbf{B}^2].\end{aligned}\tag{8}$$

When the B moments are canted, then the condition for zero torque in the exchange field requires that $\mathbf{a}_1=\mathbf{a}_2=\mathbf{a}$ and

$$\sin\psi=a/(\beta b),\tag{9}$$

where a and b are the magnitudes of the moments on the A_i and B_i subsystems and ψ is the complement of the half-angle between $\mathbf{b}_1$ and $\mathbf{b}_2$.

In most magnetic spinels, the anisotropy field is several orders of magnitude smaller than the exchange field. However, the data presented in this paper shows hausmannite to possess both a relatively large anisotropy energy and a relatively small exchange interaction, as deduced from the ferrimagnetic Curie point. Hence the validity of Eq. (9) becomes questionable, and its derivation must be modified to include the

[24] C. Zener, Phys. Rev. **96**, 1335 (1954).
[25] P. F. Bongers, thesis, Leiden, 1957 (unpublished).
[26] F. K. Lotgering, Philips Research Repts. **11**, 190 (1956).

effects of anisotropy. The appropriate generalization of the Lotgering formulation, given in Appendix II, yields

$$\sin\psi = a/[(\beta+\kappa)b], \tag{10}$$

where $\kappa = K_B/nb^2$ and $K_B \approx -0.7K_c \approx 3.3\times10^8$ ergs/mole, as shown in Appendix III. Furthermore, canted spins cannot exist, according to Appendix II, unless

$$\alpha\beta < 1-\alpha\kappa. \tag{11}$$

The asymptotic Curie temperature is related to the exchange constants by[26]

$$T_a = -n(C_A+2C_B)^{-1}(\tfrac{1}{2}C_A{}^2\alpha+3C_B{}^2\beta^*+4C_AC_B), \tag{12}$$

where C_A and C_B are the Curie constants for Mn^{2+} on A-sites and Mn^{3+} on B-sites and $\beta^* = \frac{1}{3}(4\beta-\beta')$, so that $\beta^*=\beta$ in the cubic limit and $\beta^*=\frac{2}{3}\beta$ for extreme tetragonal distortion. Taking Bongers' experimental values of $C_A=3.86$, $C_B=2.88$, and $T_a=-530°K$, we obtain

$$n = 1700/(2.48\alpha+8.30\beta^*+14.8). \tag{13}$$

With $b=2.23\times10^4$ emu/mole (see Appendix III), this yields

$$\kappa = (0.972\alpha+3.22\beta^*+5.74)\times10^{-3}. \tag{14}$$

From Appendix III, $\sin\psi \equiv \cos\bar{\psi} = 0.356$ when 4.7 μ_B is used for the moment on the A-sites ($a=1.31\times10^4$ emu/mole), this value being chosen for consistency with Bongers' observation of a nonspin-only value for C_A. Thus substitution of Eq. (14) into Eq. (10) gives $\beta=1.64$, where $\alpha\times10^{-3}$ has been neglected compared with β.

We turn next to the expression for the ferrimagnetic Curie temperature T_Δ, derived in Appendix II as Eq. (B-10). Since experimentally $T_\Delta = 41.9°K$, substitution for n, C_A, β, and κ yields $n=56$ and $\alpha=0.82$ for $\beta^*=\beta$; $n=65$ and $\alpha=0.88$ for $\beta^*=\frac{2}{3}\beta$. Therefore,

$$\alpha\beta > (0.82)(1.64) = 1.35 > 1. \tag{15}$$

This result contradicts the requirement for canted spins, given by Eq. (11).

If the spin-only values are used, then one finds ($\beta^*=\beta$) $n=53$, $\beta=1.57$, $\alpha=0.90$, and $\alpha\beta>1.42$. No significant improvement can be obtained either by using Borovik-Romanov's data[2] for T_a or by varying our experimental values well beyond the limits of experimental error. Even if the data of Jacobs[10] and Kasper[11] were ignored and the B-site moment were assumed to dominate, the resulting contradiction would be just as serious.

Given the Yafet-Kittel theory, the only possible source of error in the theoretical structure lies in the calculation of T_Δ by the molecular field approximation. Only the interaction parameter α is affected by a change in T_Δ, and it is found that a consistent value for α requires that T_Δ be raised from 41.9°K to at least 67°K if $\beta^*=\beta$, or 76°K if $\beta^*=\frac{2}{3}\beta$. The molecular field approximation can lead to errors of this magnitude when applied to systems with $J=\frac{1}{2}$,[27,28] but the error for Mn^{2+} with $J=\frac{5}{2}$ is smaller.[29] Furthermore, such an explanation for the inconsistency appears unlikely since α would be required to lie fortuitously close to its maximum allowed value and the large tetragonal distortion would be required to have negligible effect on the $B-B$ interactions.

The above analysis indicates an inability of the Yafet-Kittel theory to account simultaneously for the observed magnetization and Curie points of hausmannite. In addition, the Yafet-Kittel approach can be generalized to include 24 sublattices, one for each ion in the orthorhombic unit cell suggested by Kasper, with a variety of $A-A$, $A-B$, and $B-B$ interactions. When the search for states of minimum energy is restricted to the triangular spin configurations of the specific Yafet-Kittel model, considerable degeneracy is obtained, as shown in Appendix I. In particular, the lowest energy results from 8 configurations which do not require cell doubling, as well as from 24 which do. Within this framework, doubling does not reduce the energy. Thus the Yafet-Kittel model cannot account for the observed doubling of the unit cell.[11] Moreover, it provides no energy barriers of the type required to explain the temperature dependence of the coercive force or the dynamic properties of hausmannite.

From all the considerations given above, it follows that the Yafet-Kittel model cannot account satisfactorily for the magnetic properties of Mn_3O_4. However, Kaplan has recently shown[30] that their assumptions are overly restrictive. For a certain range of interaction strengths in cubic spinels, his results indicate that minimization of the exchange energy leads to a complex configuration of canted spins with an approximate doubling of the unit cell along any single cubic [110] direction. Since the cubic [110] is the bc tetragonal [100] his result suggests that a similar treatment of distorted spinels might account for the observed doubling of hausmannite. Furthermore, Kaplan has shown[9] that first-order pseudo-dipole anisotropy can tie the spin vectors to the propagation vector for antiferromagnetic spirals. This same effect in ferrimagnetic configurations characterized by a wave vector would give rise to an energy barrier between the bc tetragonal [100] and [010] doubling directions, in accord with the observed dynamic behavior. Although the results of Kaplan's calculations for cubic lattices are suggestive with respect to the magnetic properties of hausmannite, quantitative interpretation of our data requires an extension of his work to include tetragonally distorted spinel structures. This extension is being pursued.

---

[27] J. S. Smart, Phys. Rev. **101**, 585 (1956).
[28] P. J. Wojtowicz, J. Appl. Phys. **31**, 265S (1960).
[29] J. S. Smart, J. Phys. Chem. Solids **11**, 91 (1959).
[30] T. A. Kaplan, preceding paper [Phys. Rev., **119**, 1460 (1960)].

ACKNOWLEDGMENTS

We wish to express our gratitude to D. M. Seaman of the New York Museum of Natural History and to Professor C. Frondel of the Peabody Museum of Harvard University for giving us the hausmannite single crystals, to J. W. Sanchez and R. Arnott for orienting these crystals, and to D. G. Wickham for supplying the polycrystalline samples. We are also indebted to I. S. Jacobs and J. S. Kasper for many helpful discussions as well as for preprints of their papers. We wish to thank T. A. Kaplan both for his encouragement on all phases of this study and for explanations of his calculations on cubic spinels, and to thank J. B. Goodenough for discussions on the electronic configuration of octahedral Mn^{3+} ions.

APPENDIX I

We wish to generalize the specific Yafet-Kittel model to a tetragonally distorted spinel with an orthorhombic, doubled unit cell. The complete molecular-field calculation then involves eight A-site sublattices and sixteen B-site sublattices, with respective magnetizations $\mathbf{a}_i$ and $\mathbf{b}_j$. There are five distinct interaction strengths for nearest-neighbor pairs: n_1 for the four A_i-B_j pairs lying close to the c axis, n_2 for the other eight A_i-B_j pairs, β_1 for the two B_i-B_j pairs lying in a c plane, β_2 for the other four B_i-B_j pairs, and α_1 for the four A_i-A_j pairs. With these definitions, the molecular fields can be written as

$$\begin{aligned}-\mathbf{h}_{Ai}&=\alpha_1\textstyle\sum_k{}'^i\,\mathbf{a}_k+n_1\sum_k{}'^i\,\mathbf{b}_k+n_2\sum_k{}''^i\,\mathbf{b}_k\\ -\mathbf{h}_{Bj}&=n_1\textstyle\sum_k{}'^j\mathbf{a}_k+n_2\sum_k{}''^j\,\mathbf{a}_k\\ &\quad+\beta_1\textstyle\sum_k{}'^j\mathbf{b}_k+\beta_2\sum_k{}''^j\,\mathbf{b}_k,\end{aligned}\tag{A-1}$$

where $\sum_k{}'^i$ and $\sum_k{}''^i$ denote sums over the appropriate nearest neighbors for each A_i, and similarly for the B_j sublattices. The exchange energy is given by

$$E_{\rm ex}=-\tfrac{1}{2}[\textstyle\sum_i\mathbf{a}_i\cdot\mathbf{h}_{Ai}+\sum_j\mathbf{b}_j\cdot\mathbf{h}_{Bj}],\tag{A-2}$$

where i runs from 1 to 8 and j from 1 to 16. The true minimization of this energy lies outside the scope of the triangular spin arrangements of the Yafet-Kittel model, and will be the subject of a later investigation.

The Yafet-Kittel theory predicts that the $\mathbf{a}_i$ moments must all be parallel when the $\mathbf{b}_j$ are canted. By inverting this prediction into an imposed constraint, we obtain a restricted form of Eq. (A-2) which is the desired generalization of the specific Yafet-Kittel model. Equilibrium under the imposed constraints yields seven relationships among the $\mathbf{b}_j$. These further reduce the complexity of Eq. (A-2), so that the exchange energy, after some straightforward but tedious algebra, can be written as

$$\begin{aligned}E_{\rm ex}=2\alpha_1\textstyle\sum_i(\mathbf{a}_i);&-\beta_1\sum_j(\mathbf{b}_j)^2+2(n_1+2n_2)\mathbf{a}_i\cdot\mathbf{B}\\ &+\beta_2\textstyle\sum_r(\mathbf{B}_r)^2+(\beta_1-\beta_2)\sum_r\sum_s(\mathbf{B}_{rs})^2.\end{aligned}\tag{A-3}$$

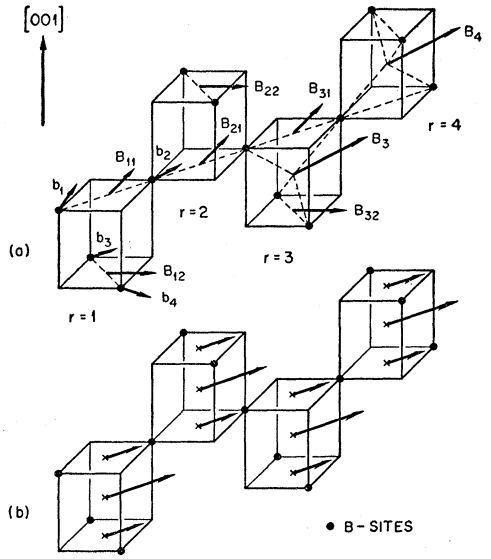

FIG. 7. Illustration of the grouping of B-sites into subcells. (a) Definitions of $\mathbf{B}_{rs}$ as the resultant moment of two nearest neighbors in the same c plane and of $\mathbf{B}_r$ as the resultant moment of a subcell. (b) Relationships between the $\mathbf{B}_{rs}$ and $\mathbf{B}_r$ given by the solution of Eq. (A-3) for hausmannite, e.g., for $\beta_1>\beta_2$.

Because of the relationships among the $\mathbf{b}_j$ due to the imposed constraints, the four B-sites in one chain along the direction of orthorhombic doubling of the unit cell can be omitted, with the four sites in the other chain counted twice. This permits a grouping of the B-sites into four subcells forming a chain along the doubled direction, as illustrated in Fig. 7(a). Thus, in Eq. (A-3), $\mathbf{B}_{rs}$ is the resultant moment of two B-sites which lie in the same c plane ($s=1,2$) in the rth subcell; $\mathbf{B}_r$ is the resultant moment of the four B-sites in the rth subcell, $\mathbf{B}_r=\sum_s\mathbf{B}_{rs}$; and $\mathbf{B}$ is the resultant moment of all the B-site sublattices, $\mathbf{B}=\sum_r\mathbf{B}_r=\sum_j\mathbf{b}_j$.

To minimize Eq. (A-3), we first chose any permissible value for $\mathbf{B}$ and four arbitrary values for the $\mathbf{B}_r$ such that $\sum_r\mathbf{B}_r=\mathbf{B}$. With these specific choices, the lowest possible energy is obtained by minimizing the fifth term of Eq. (A-3). If $\beta_1>\beta_2$, $\sum_r\sum_s(\mathbf{B}_{rs})^2$ must be a minimum; if $\beta_1<\beta_2$, it must be a maximum. Since the $\mathbf{B}_r=\sum_s\mathbf{B}_{rs}$ have been fixed, the two extrema, respectively, require $\mathbf{B}_{rs}=\frac{1}{2}\mathbf{B}_r$ or $\mathbf{B}_{rs}=2\mathbf{b}_j$. The former case corresponds to hausmannite and is illustrated in Fig. 7(b). The latter case requires all the $\mathbf{b}_j$ in a plane to be parallel, corresponding to copper chromite.[13]

With $\mathbf{B}_{rs}=\frac{1}{2}\mathbf{B}_r$, we can rewrite Eq. (A-3) in the form

$$\begin{aligned}E_{\rm ex}=16\alpha_1\mathbf{a}_i{}^2-16\beta_1\mathbf{b}_j{}^2+2(n_1+2n_2)\mathbf{a}_i\cdot\mathbf{B}\\ +\tfrac{1}{2}(\beta_1+\beta_2)\textstyle\sum_r(\mathbf{B}_r)^2.\end{aligned}\tag{A-4}$$

If any arbitrary fixed value is assumed for $\mathbf{B}=\sum_r\mathbf{B}_r$, then the lowest energy is obtained when $\sum_r(\mathbf{B}_r)^2$ is a minimum. This condition requires $\mathbf{B}_r=\frac{1}{4}\mathbf{B}$, so that

Eq. (A-4) becomes

$$E_{ex}=16\alpha_1\mathbf{a}_i^2-16\beta_1\mathbf{b}_j^2+2(n_1+2n_2)\mathbf{a}_i\cdot\mathbf{B}+\tfrac{1}{8}[\beta_1+\beta_2)\mathbf{B}^2. \quad \text{(A-5)}$$

Because of its relationship to $\mathbf{B}_{rs}$, the net moment $\mathbf{B}$ is parallel to the resultant moment of any c-plane nearest-neighbor pair, and its magnitude depends only on the half-angle $\bar{\psi}$ between the moments of two such neighbors. Hence Eq. (A-5) can be solved uniquely for this angle $\bar{\psi}$.

From the discussion above, it is evident that, for fixed interaction strengths and fixed sublattice magnetizations, the exchange energy of Eq. (A-3) depends only on the resultant moments of c-plane nearest neighbor pairs. Hence the unique lowest energy can be obtained with many possible orientations of the individual moments compatible with the required resultant, i.e., the ground state is highly degenerate. If the $\mathbf{b}_j$ are all restricted to lie in a particular plane and one $\mathbf{b}_j$ is fixed, then the lowest energy results from any of 32 distinct ways of ordering independent pairs. Only 24 of these configurations yield a doubled unit cell. Hence the particular configuration suggested by Kasper[11] is degenerate not only with other arrangements requiring a doubled cell, but also with ones which do not cause doubling.

Any molecular field calculation will necessarily give the same results for any of these degenerate ground states. Moreover, the 32 configurations mentioned above include two which correspond to the same six sublattices considered by Lotgering.[26] Because of this twofold degeneracy, the four B-lattices reduce to two B-subsystems, and the molecular fields can be expressed in terms of the resultant A-site moment $\mathbf{A}=\sum_i\mathbf{a}_i$, the moments on two A-site subsystems $\mathbf{a}_k=4\mathbf{a}_i(|\mathbf{a}_k|=a)$, the resultant B-site moment $\mathbf{B}=\sum_j\mathbf{b}_j$, and the moments on the two B-site subsystems $\mathbf{b}_k=8\mathbf{b}_j(|\mathbf{b}_k|=b)$. The molecular fields given in Eq. (A-1) can then be reformulated within the framework of the Lotgering notation, as given by Eq. (7), with $n=\frac{1}{4}(n_1+2n_2)$, $n\alpha=\alpha_1$, $n\beta=\frac{1}{4}(\beta_1+\beta_2)$, and $n\beta'=\frac{1}{2}\beta_1$ for hausmannite [$n\beta=\frac{1}{2}\beta_2$, $n\beta'=\frac{1}{2}(2\beta_2-\beta_1)$ for copper chromite], and Eq. (8) is identical with Eq. (A-5). The only difference between the original formulation[26] and Eqs. (7) and (8) lies in the distinction between β and β' arising from the tetragonal distortion. The preceeding discussion shows that, once this distinction is made, the Lotgering analysis is completely applicable to hausmannite with its tetragonal distortion and orthorhombic, doubled unit cell.

APPENDIX II

We wish to include the anisotropy energy in a molecular-field calculation for canted spins, assuming that only the B-sites have angled moments and that they are coplanar with the c axis and the A-site moment. However, we do not assume a rigid system, i.e., the net B-site moment $\mathbf{B}$ need not be colinear with the net A-site moment $\mathbf{A}$ when external fields are applied. Figure 8 shows a possible configuration and defines the angles used in this analysis. Explicit evaluation of Eqs. (7) and (8) in terms of these angles yields

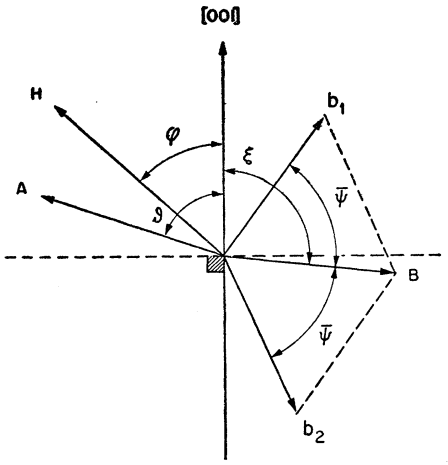

FIG. 8. Definition of angular coordinates used in this analysis. $\mathbf{b}_1$ and $\mathbf{b}_2$ are the individual B-site moments, $\mathbf{B}$ is their vector sum, and $\mathbf{A}$ is the net A-site moment. In Appendix II, we further define $\xi-\frac{1}{2}\pi=\delta$ and $\frac{1}{2}\pi-\varphi=\delta+\epsilon$.

$$E_{ex}=\alpha na^2-\tfrac{1}{2}\beta' nb^2+2\beta nb^2\cos^2\bar{\psi}+4nab\cos\bar{\psi}\cos(\vartheta+\xi), \quad \text{(B-1)}$$

and the magnetic energy in an external field is given by

$$E_H=-2aH\cos(\varphi-\vartheta)-2bH\cos\bar{\psi}\cos(\varphi+\xi). \quad \text{(B-2)}$$

In order to write down the anisotropy energy, we introduce two positive anisotropy constants K_A and K_B for the A- and B-sites so that

$$E_K=K_A\cos^2\vartheta+K_B[\sin^2(\xi-\bar{\psi})+\sin^2(\xi+\bar{\psi})]. \quad \text{(B-3)}$$

The sum of these three energies constitute the total energy, $E=E_{ex}+E_H+E_k$.

For equilibrium, the derivatives $\partial E/\partial\vartheta$, $\partial E/\partial\xi$, and $\partial E/\partial\bar{\psi}$ must all vanish, giving, respectively,

$$0=4nab\cos\bar{\psi}\sin(\vartheta+\xi)+K_A\sin2\vartheta+2aH\sin(\varphi-\vartheta), \quad \text{(B-4a)}$$

$$0=4nab\cos\bar{\psi}\sin(\vartheta+\xi)-2K_b\sin2\xi\cos2\bar{\psi}-2bH\cos\bar{\psi}\sin(\varphi+\xi), \quad \text{(B-4b)}$$

$$0=4nab\sin\bar{\psi}\cos(\vartheta+\xi)+2\beta nb^2\sin2\bar{\psi}-2K_b\cos2\xi\sin2\bar{\psi}-2bH\sin\bar{\psi}\cos(\varphi+\xi). \quad \text{(B-4c)}$$

For an external field perpendicular to the c axis, $\varphi=\frac{1}{2}\pi$, and the solution of Eq. (B-4) gives $\vartheta=\xi=\frac{1}{2}\pi$ and

$$\sin\psi\equiv\cos\bar{\psi}=(nab-\tfrac{1}{2}bH)/(\beta nb^2+K_B)=(a-\tfrac{1}{2}H/n)/[b(\beta+\kappa)], \quad \text{(B-5)}$$

where κ is written for $K_B/(nb^2)$. Assuming that the A-site moment dominates,[10] the net magnetization is

$M=2a-2b\sin\psi$. From this relation together with Eq. (B-5), we find the high-field susceptibility to be

$$\chi=\partial M/\partial H=[n(\beta+\kappa)]^{-1}. \quad \text{(B-6)}$$

Furthermore, in the absence of an external field, Eq. (B-5) becomes

$$\sin\psi\equiv\cos\bar{\psi}=a/[b(\beta+\kappa)]. \quad \text{(B-7)}$$

The energy for the canted spin arrangement in zero field can be obtained by substituting from Eq. (B-7) into Eqs. (B-1) and (B-3);

$$E_\Delta=\alpha na^2-\tfrac{1}{2}\beta' nb^2-2na^2/(\beta+\kappa). \quad \text{(B-8)}$$

If the moments on the two kinds of A-sites and on the two kinds of B-sites are separately antiparallel, then the total energy $E=-\alpha na^2-\frac{1}{2}\beta' nb^2$. Comparison of this energy with E_Δ shows that canted spins cannot exist unless

$$\alpha(\beta+\kappa)<1. \quad \text{(B-9)}$$

On the basis of Jacobs' findings[10] it is reasonable to assume that hausmannite passes from the ferrimagnetic state into one where the A-sites are paramagnetic with antiferromagnetic B-sites, before reaching a truly paramagnetic state. According to this assumption, the A-site moment vanishes at the ferrimagnetic Curie point T_Δ, so that the molecular field approximation gives $M_A=(C_A/T_\Delta)|\mathbf{h}_A|$. Using Eqs. (7) and (B-7) with the definition of $\bar{\psi}$ to evaluate $|\mathbf{h}_A|$, we find

$$T_\Delta=nC_A[(\beta+\kappa)^{-1}-\tfrac{1}{2}\alpha] \quad \text{(B-10)}$$

since $M_A=2a$ and $M_B=b$ as shown by Lotgering.[26]

APPENDIX III

To determine the relationship between the observed anisotropy K_c and the anisotropies K_A and K_B introduced in Appendix II, we must consider the general case of an arbitrarily directed external field. Let $\xi=\frac{1}{2}\pi+\delta$ and $\vartheta=\frac{1}{2}\pi-\delta-\epsilon$, where the angle δ represents a rigid rotation and ϵ represents the deviation from rigidity. When ϵ is assumed to be small, only the first terms in the expansions for $\sin\epsilon$ and $\cos\epsilon$ need be retained. The difference between Eqs. (B-4a) and (B-4b) then becomes

$$2aH[\cos(\varphi+\delta)-\epsilon\sin(\varphi+\delta)]-K_A(2\epsilon\cos2\delta+\sin2\delta)=2bH\cos\bar{\psi}\cos(\varphi+\delta)-2K_B\sin2\delta\cos2\bar{\psi}. \quad \text{(C-1)}$$

Similarly, Eqs. (B-4b) and (B-4c) can be rewritten as

$$0=2nab\epsilon\cos\bar{\psi}+K_B\sin2\delta\cos2\bar{\psi}-bH\cos\bar{\psi}\cos(\varphi+\delta), \quad \text{(C-2)}$$

$$0=[-2nab+bH\sin(\varphi+\delta)+2(\beta nb^2+K_B\cos2\delta)\cos\bar{\psi}]\sin\bar{\psi}. \quad \text{(C-3)}$$

From Eq. (B-3) it follows that

$$\cos\bar{\psi}=[a-\tfrac{1}{2}n^{-1}H\sin(\varphi+\delta)]/[b(\beta+\kappa\cos2\delta)], \quad \text{(C-4)}$$

where $\kappa=K_B/(nb^2)$. Comparison with Eq. (B-5) shows that the high-field susceptibility depends essentially upon the component of H along the net magnetization, with a small correction in the denominator to account for the varying effectiveness of the anisotropy. From Eq. (C-2) one obtains

$$2a\epsilon=-b\kappa\sin2\delta\cos2\bar{\psi}\sec\bar{\psi}+n^{-1}H\cos(\varphi+\delta), \quad \text{(C-5)}$$

which yields, upon substitution into Eq. (C-1),

$$\{K_B(nab)^{-1}\cos2\bar{\psi}\sec\bar{\psi}[K_A\cos2\delta+aH\sin(\varphi+\delta)]-K_A+2K_B\cos2\bar{\psi}\}\sin2\delta=H\cos(\varphi+\delta)\{2b\cos\bar{\psi}-2a+b(nab)^{-1}[K_A\cos2\delta+aH\sin(\varphi+\delta)]\}. \quad \text{(C-6)}$$

When $\epsilon=0$, the terms in the square brackets cancel. In the general case ($\epsilon\neq0$), these terms are of the order of an anisotropy energy K_A and a magnetic energy aH, and are divided by a factor nab, which is an exchange energy. Assuming that $K_A/(nab)\ll1$ and $aH/(nab)\ll1$, it follows that

$$\sin2\delta\cong(2a-2b\cos\bar{\psi})(K_A-2K_B\cos2\bar{\psi})^{-1}H\cos(\varphi+\delta)=(K_A-2K_B\cos2\bar{\psi})^{-1}HM\cos(\varphi+\delta). \quad \text{(C-7)}$$

For the experimental anisotropy, equilibrium is given by Eq. (3). Putting $\vartheta_c=\frac{1}{2}\pi=\delta$, we can rewrite this equation in the form

$$\sin2\delta=(-K_c)^{-1}HM\cos(\varphi+\delta), \quad \text{(C-8)}$$

so that comparison with Eq. (C-7) yields

$$-K_c\cong K_A-2K_B\cos2\bar{\psi}. \quad \text{(C-9)}$$

Because the tetragonal distortion arises from the Mn^{3+} ions on the B-sites, it is reasonable to attribute almost all of the anisotropy to K_B. In order to evaluate $\cos\bar{\psi}=(2b)^{-1}(2a-M)$, we need the molar values, which are given[26] by: $b=N\mu_B g j_B=2.23\times10^4$ emu/mole, $a=\frac{1}{2}N\mu_B g j_A=1.40\times10^4$ emu/mole for spin-only, and $a=1.31\times10^4$ emu/mole for 4.7 μ_B, as is frequently observed for Mn^{2+} ions on A-sites. Experimentally, $M=1.85\ N\mu_B=1.034\times10^4$ emu/mole, so that $\cos\bar{\psi}=0.396$ for spin-only and $\cos\bar{\psi}=0.356$ for 4.7 μ_B on the A-sites. In either case, $\cos2\bar{\psi}\cong-0.7$ and $K_B\approx-0.7K_c\approx0.7\times10^7$ ergs/cc $\approx3.3\times10^8$ ergs/mole.

Finally, the approximation used in deriving Eq. (C-7) must be examined. Taking $n\cong50$, the term $nab\cong15\times10^9$ ergs/mole. Consequently $K_B/(nab)\approx0.02$, so that little error will be caused by neglecting $K_A/(nab)$ even if K_A is not much smaller than K_B. For $H=10^4$ oe, $aH/(nab)\approx0.01$ and its neglect will similarly not cause appreciable error.